

1 **Protein-carbohydrate ingestion alters Vps34 cellular localization independent of changes in**
2 **kinase activity in human skeletal muscle**

3 Nathan Hodson^{1#}, Jessica R. Dent^{1#}, Zhe Song¹, Mary F. O’Leary¹, Thomas Nicholson², Simon
4 W. Jones², James T. Murray³, Stewart Jeromson⁴, D. Lee Hamilton⁵, Leigh Breen¹, Andrew
5 Philp^{1,6,7}.

6 1. School of Sport, Exercise and Rehabilitation Sciences, University of Birmingham, UK.

7 2. Institute of Inflammation and Ageing, University of Birmingham, UK.

8 3. Trinity Biomedical Sciences Institute, Trinity College, Dublin, Ireland.

9 4. Physiology, Exercise and Nutrition Research Group, School of Sport, Faculty of Health,
10 Stirling University, Stirling, UK.

11 5. Institute for Physical Activity and Nutrition (IPAN), School of Exercise & Nutrition
12 Sciences, Deakin University, Geelong 3216, Australia.

13 6. Garvan Institute of Medical Research, NSW, Australia.

14 7. St Vincent’s Clinical School, UNSW Medicine, UNSW Sydney, NSW, Australia.

15 * Corresponding author:

16 Andrew Philp, Ph.D.

17 Mitochondrial Metabolism and Ageing Laboratory

18 Healthy Ageing Theme

19 Garvan Institute of Medical Research

20 384 Victoria Street, Darlinghurst, NSW, 2010, Australia

21 Phone: +61 (0) 292958249

Email: a.philp@garvan.org.au

22 [#]Authors contributed equally

23

24 **Abstract**

25 The mechanistic target of rapamycin (mTOR) complex 1 (mTORC1) regulates cell size and
26 growth in response to nutrients, however, the mechanisms by which nutrient levels are sensed by
27 mTORC1 in human skeletal muscle are yet to be fully elucidated. The Class III PI3Kinase Vps34
28 has recently been proposed as a sensor essential for mTORC1 activation following nutrient
29 stimulation. We therefore investigated the effects of increasing nutrient availability through
30 protein-carbohydrate (PRO-CHO) feeding on Vps34 kinase activity and cellular localization in
31 human skeletal muscle. Eight young, healthy males (age – 21 ± 0.5 yrs, mean \pm SEM) ingested a
32 PRO-CHO beverage containing 20/44/1g PRO/CHO/FAT respectively, with skeletal muscle
33 biopsies obtained at baseline and 1h and 3h post-feeding. PRO-CHO feeding did not alter Vps34
34 kinase activity, but did stimulate Vps34 translocation toward the cell periphery (PRE
35 (mean \pm SEM) - 0.273 ± 0.021 , 1h - 0.347 ± 0.022 , Pearson's Coefficient (r)) where it co-localized
36 with mTOR (PRE – 0.312 ± 0.018 , 1h – 0.348 ± 0.024 , Pearson's Coefficient (r))). These
37 alterations occurred in parallel to an increase in S6K1 kinase activity – $941 \pm 164\%$ of PRE at 1h
38 post-feeding). Subsequent *in vitro* experiments in C2C12 and human primary myotubes
39 displayed no effect of the Vps34-specific inhibitor SAR405 on mTORC1 signalling responses to
40 elevated nutrient availability. Therefore, in summary, PRO-CHO ingestion does not increase
41 Vps34 activity in human skeletal muscle, whilst pharmacological inhibition of Vps34 does not
42 prevent nutrient stimulation of mTORC1 *in vitro*. However, PRO-CHO ingestion promotes
43 Vps34 translocation to the cell periphery, enabling Vps34 to associate with mTOR. Therefore,
44 our data suggests that interaction between Vps34 and mTOR, rather than changes in Vps34
45 activity *per se* may be involved in PRO-CHO activation of mTORC1 in human skeletal muscle.

46 **Introduction**

47 Amino acids (AAs) are critical to skeletal muscle plasticity, acting as both substrates in the
48 process of muscle protein synthesis (MPS) as well as initiating the signaling pathways which
49 activate this cellular process (32, 33). Carbohydrate (CHO) ingestion can also elevate MPS via
50 insulin action (3), and a combination of these nutrients is believed to act synergistically on MPS
51 following exercise (20). In skeletal muscle, it is believed that increases in MPS are governed
52 primarily by the activation of the mechanistic target of rapamycin complex 1 (mTORC1) (5, 6),
53 an evolutionarily conserved serine/threonine kinase complex which stimulates translation
54 initiation and elongation (14, 16, 31) in response to increased nutrient provision.

55 The canonical mechanism by which AAs stimulate mTORC1 activity is thought to be through
56 the elevation of mTORC1 complex co-localization with the lysosome (27) *in vitro*, or through
57 mTORC1/lysosomal trafficking *in vivo/vitro* (11, 15, 28). However, how nutrients stimulate
58 mTORC1 activity in human skeletal muscle is still poorly understood. A potential nutrient-
59 sensitive activator of mTORC1 is the vacuolar protein sorting 34 (Vps34), a class III PI3Kinase.
60 The primary function of Vps34 is the production of phosphatidylinositol 3-phosphate (PI(3)P)
61 through the phosphorylation of phosphatidylinositol (2), a product responsible for the
62 recruitment of various proteins to phospholipid bilayers (i.e. plasma and lysosomal membranes)
63 (8). A role for Vps34 in nutrient sensing was first proposed by Byfield et al. (4), who reported
64 that overexpression of Vps34 in HEK293 cells elicited a 2-fold increase in S6K1 activity, a
65 common readout of mTORC1 activation. Conversely, siRNA targeting Vps34 abolished insulin-
66 stimulated S6K1^{Thr389} phosphorylation (4). Nobukuni et al. (22) reiterated these findings,
67 displaying that siRNA-mediated reductions in Vps34 expression, in HEK293 cells, dramatically
68 attenuated mTORC1 activation in response to both AA and insulin stimulation. In addition,

69 recent *in vitro* evidence suggests that Vps34 colocalises with mTOR, close to cellular
70 membranes, following insulin stimulation (10), and is required for nutrient-stimulated
71 translocation and activation of mTORC1 (10). As such, Vps34 represents a novel candidate as a
72 nutrient-sensitive activator of mTORC1.

73 With regard to skeletal muscle, 3h and 24h exposure to leucine (5mM) and insulin (100nM)
74 elevated Vps34 protein content and mTOR^{Ser2448} and S6K1^{Thr389} phosphorylation in human
75 primary myotubes (9), whilst supra-physiological levels of AA's increases Vps34 activity in
76 C2C12 myotubes (17). In addition, high frequency electrical contraction has been reported to
77 increase Vps34 activity in rodent *Tibialis Anterior* muscle (17), whereas sprint exercise and
78 protein ingestion failed to activate Vps34 in human skeletal muscle (26). Overall, such data
79 implicates a possible role for Vps34 in nutrient/contraction sensing within skeletal muscle.
80 However, a more detailed investigation in human skeletal muscle is required.

81 Therefore, our primary aim was to investigate if AA/CHO feeding could affect Vps34 activity
82 and cellular localisation in human skeletal muscle. We hypothesised that Vps34 activity would
83 increase in response to AA/CHO feeding in parallel to increases in mTORC1 signaling. Our
84 secondary aim was to examine whether inhibition of Vps34 kinase activity *in vitro* with the
85 specific inhibitor SAR405 (24, 25) would attenuate nutrient-activation of mTORC1.

86 **Methods**

87 *Participants*

88 Eight young, healthy males (age – 21 ± 0.5yrs, mean ± SEM) volunteered to partake in the
89 current study. All participants were considered healthy (as assessed by a general health
90 questionnaire) and recreationally active (~3 exercise sessions per week) but not involved in a

91 structured exercise training program. Exclusion criteria encompassed current cigarette smokers,
92 recreational drug users (including anabolic steroids), the presence of neuromuscular disease and
93 any medication/condition that may affect nutrient digestion/absorption i.e. inflammatory bowel
94 disease. Participants provided written informed consent prior to participation and all procedures
95 were approved by the NHS West Midlands Black Country Research Ethics Committee
96 (15/WM/0003) and conformed to the standards set out in the Declaration of Helsinki (7th
97 version).

98 *Study Design*

99 On the day of the experimental trial, participants reported to the laboratory following an
100 overnight fast (~10h) and having refrained from strenuous exercise and alcohol consumption in
101 the prior 48h. Upon arrival, participants were placed in a supine position and a 21G cannula was
102 inserted into the antecubital vein of one arm to allow for repeated blood sampling. At this point
103 an initial baseline blood sample was obtained from all participants. A skeletal muscle biopsy
104 sample was then taken from the *vastus lateralis* of a randomised leg using the Bergstrom
105 percutaneous needle technique, modified for suction (30). Participants then consumed a
106 commercially available protein-carbohydrate beverage (Gatorade Recover®, Gatorade, Chicago,
107 IL, USA.) providing 20/44/1g of protein, carbohydrate and fat respectively. Further venous blood
108 samples were taken every 20 minutes for a 3h post-prandial period and subsequent skeletal
109 muscle biopsy samples were obtained at 1h and 3h following beverage ingestion. Muscle
110 samples were blotted free of excess blood and dissected free of any excess adipose and
111 connective tissue, then immediately frozen in liquid nitrogen and stored at -80°C until analysis.
112 A separate piece of muscle tissue was placed in optimal cutting temperature (OCT) compound
113 (VWR, Lutterworth, UK.) and frozen in liquid nitrogen-cooled isopentane before storage at -

114 80°C. Blood samples were collected into EDTA-coated vacutainers (BD, Franklin Lakes, NJ,
115 USA.) and then centrifuged at 1000g for 15min to separate plasma. Plasma was then aliquotted
116 into micro-centrifuge tubes and stored at -80°C until analysis. The experimental design is
117 depicted in Figure 1.

118 *Blood analyses*

119 Plasma insulin concentrations were quantified using a commercially-available ELISA kit (IBL
120 International, Hamburg, Germany.) as per the manufacturer's instructions. Plasma leucine
121 concentrations were determined via gas chromatography-mass spectrometry (GC-MS) using an
122 internal standard method, as previously described (19), following the conversion of plasma free
123 amino acids to their N-tert-butyl-dimethyl-silyl-N-methyltrifluoroacetamide (MTBSTFA)
124 derivative.

125 *S6K1 and AKT Kinase Activity Assays*

126 S6K1 and AKT kinase activity assays were conducted as described previously (18) with the
127 following antibodies; S6K1 – SCBT no.2708 (Santa Cruz Biotechnologies, Dallas, TX, USA.) &
128 AKT (DSTT, Dundee, UK). Briefly, a ~30mg piece of muscle tissue was homogenized on ice in
129 RIPA buffer (50 mmol/l Tris-HCl pH 7.5, 50 mmol/l NaF, 500 mmol/l NaCl, 1 mmol/l sodium
130 vanadate, 1 mmol/l EDTA, 1% (vol/vol) Triton X-100, 5 mmol/l sodium pyrophosphate, 0.27
131 mmol/l sucrose, and 0.1% (vol/vol) 2-mercaptoethanol and Complete protease inhibitor cocktail
132 (Roche)). Cellular debris was then removed via centrifugation at 13000g for 15min (4°C).
133 Protein concentrations of samples was then determined via bicinchoninic acid (BCA) protein
134 assay. Immunoprecipitation of the target protein was then conducted on 200µg protein for 2h at
135 4°C in homogenization buffer (50 mM Tris-HCl pH 7.5, 0.1 mM EGTA, 1 mM EDTA, 1%

136 (vol/vol) Triton X-100, 50 mM NaF, 5 mM NaPPi, 0.27 M sucrose, 0.1% β -mercaptoethanol, 1
137 mM Na₃(OV)₄, and 1 Complete (Roche) protease inhibitor tablet per 10 mL) combined with
138 2.5 μ L Protein G Sepharose beads and appropriate antibody. Immunoprecipitates were
139 subsequently washed twice in high-salt buffer (homogenization buffer with 0.5M NaCl added)
140 and once in assay buffer (50 mM Tris·HCl pH 7.4, 0.03% Brij35, and 0.1% β -mercaptoethanol).
141 Immunoprecipitates were then resuspended in 10 μ L assay buffer and activity assay commenced
142 every 20 seconds through the addition of a hot assay mix (assay buffer + 100 μ M ATP + 10mM
143 MgCl₂ + 32 γ ATP + synthetic substrate (S6tide - KRRRLASLR at 30 μ M & Crosstide -
144 GRPRTSSFAEG at 30 μ M for S6K1 and AKT assays respectively). Every 20s reactions were
145 stopped through spotting on to chromatography paper, immersion in 75mM phosphoric acid and
146 drying. Chromatography paper was immersed in GoldStar LT Quinta Scintillation fluid
147 (Meridian Biotechnologies, Chestfield, UK) and spots were counted in a Packard 2200CA
148 TriCarb Scintillation Counter (United Technologies) as fmol·min⁻¹·mg⁻¹.

149 *Vps34 Kinase Activity Assay*

150 Vps34 kinase activity assays were conducted as previously described (17) from 25mg muscle
151 homogenized in Cantley lysis buffer. Vps34 was immunoprecipitated overnight at 4°C from
152 tissue lysates containing ~1mg total protein using 2 μ g anti-Vps34 antibody (sheep antibody
153 produced by Dr. James T. Murray, Trinity College Dublin) before immobilisation on Protein G
154 Sepharose beads for 1h. Immunoprecipitates were then washed 3 times in Cantley lysis buffer,
155 once in Tris-LiCl (10 mM Tris, pH 7.5, 5 mM LiCl, 0.1 mM Na₂VO₄) and twice in TNE (10
156 mM Tris, pH 7.5, 150 mM NaCl, 1 mM EDTA, 0.1 mM Na₂VO₄) and then resuspended in 60 μ L
157 TNE+ (TNE, 0.5 mM EGTA, pH 8.0, 1 : 1000 2-mercaptoethanol). Samples were then incubated
158 with 20 μ g Vps34 antigen peptide for 10min before 10 μ L of 30 mM MnCl₂ and 10 μ L of 2 mg

159 ml⁻¹ phosphoinositol were added to provide substrate for the reaction. Reactions then
160 commenced through the addition of 5 μ L assay buffer (400 μ M unlabelled ATP, 12.5 μ Ci of
161 ³² γ ATP, 4.3 μ l water) for 10 minutes at 30°C. Reactions were terminated by the addition of
162 20 μ L 8M HCl, phase separated using 1:1 chloroform and methanol and the lower phase spotted
163 onto an aluminium-backed 60 A silica ° TLC plate (Merck, Damstadt, Germany). This was then
164 run in a TLC chamber solvent system to determine ³² γ P transfer to substrate.

165 *Immunohistochemistry*

166 Immunohistochemical analysis was conducted as described previously (28). In short, 5 μ m
167 sections of muscle tissue were sectioned at -25°C using a Bright 5040 Cryostat (Bright
168 Instrument Company Ltd., Huntingdon, UK) and transferred to room temperature (RT) glass
169 slides (VWR international, UK) and allowed to air-dry for ~1h. Sections from each time point for
170 each participant were sectioned onto the same slide in duplicate to remove slide-to-slide
171 variation during analysis. Muscle sections were subsequently fixed in a 3:1 solution of acetone
172 and ethanol, washed 3 times in Phosphate Buffered Saline (PBS) before incubation in relevant
173 primary antibodies (antibodies and dilutions in Table 1) diluted in 5%NGS to prevent non-
174 specific secondary binding for 2h at RT. Subsequently, sections were again washed in PBS and
175 then incubated in corresponding secondary antibodies (details in Table 1) for 1h at RT.
176 Following further washes, slides were then incubated in Wheat Germ Agglutinin (WGA –
177 conjugated to 350nm fluorophore) for 30min at RT in order to mark the sarcolemmal membrane.
178 After a final wash in PBS, slides were then mounted in Mowiol® 4–88 (Sigma-Aldrich, Poole,
179 UK) to protect fluorophores and a glass coverslip was applied. Slides were then left to dry
180 overnight in a dark cabinet prior to image capture. Pilot stains were also conducted with and

181 without the presence of the Vps34 primary antibody to ensure no non-specific binding of the
182 secondary antibody.

183 *Image Capture and Analysis*

184 Stained muscle sections were observed under a Nikon E600 widefield microscope using a
185 40x0.75NA objective under three colour filters achieved by a SPOT RT KE colour three shot
186 CCD camera (Diagnostic Instruments Inc., MI, USA) illuminated by a 170W Xenon light source.
187 In the current study, DAPI UV (340-380nm) excitation filter was utilized to visualize WGA,
188 TxRed (540-580nm) for mTOR visualization and FITC (465-495nm) for LAMP2.Vps34
189 depending on the stain conducted. For each time point, approximately 8 images were taken per
190 section, each consisting of ~8 muscle fibers. As sections were analysed in duplicate,
191 approximately 120 muscle fibres per time point per participant were included in analysis. Image
192 processing and quantification was completed on ImageProPlus 5.1 software (Media Cybernetics,
193 MD, USA.) with all variables kept consistent for all sections on a given slide. Prior to co-
194 localisation analysis, all images underwent a no neighbour deconvolution algorithm as a filter.
195 Pearson's correlation coefficient (Image-Pro software) was used to quantify co-localization of
196 proteins stained in different channels. This method of assessing co-localization was utilized as it
197 measures co-localization on a pixel-by-pixel basis and is relatively free of user bias (7).

198 *In vitro experiments*

199 C2C12 myoblasts were purchased from American Type Culture Collection (ATCC, Manassas,
200 VA, USA.) and cultured on 150mm culture plates in high glucose Dulbecco's minimum essential
201 medium (DMEM, ThermoFisher Scientific, Waltham, MA, USA.) supplemented with 10%
202 foetal bovine serum (FBS, Hyclone, VWR, Lutterworth, UK.) and 1% penicillin-streptomycin

203 (PS, ThermoFisher Scientific). When 80% confluent, cells were trypsinized (0.05% Trypsin-
204 EDTA, ThermoFisher Scientific) and seeded onto 6-well plates at a density of 2×10^5 cells/well.
205 Myoblasts were then cultured until ~95% confluency (~36h) at which time media was changed
206 to elicit differentiation of myoblasts to myotubes (DMEM supplemented with 2% horse serum
207 (HS, Hyclone, VWR) and 1% PS). Differentiation was allowed to occur for 5 days, with media
208 replaced every other day, until myotubes were fully formed.

209 At this point, myotubes were nutrient deprived in Earl's Balanced Salt Solution (EBSS,
210 ThermoFisher Scientific) for ~14h, with a subset of myotubes maintained in DMEM (2% HS,
211 1% PS) to serve as a 'baseline' condition. Following nutrient deprivation, a subset of myotubes
212 were collected and the remaining myotubes were split into 2 conditions, serum recovery and
213 serum recovery + Vps34 inhibition. Vps34 inhibition was achieved via the addition of the
214 specific Vps34 inhibitor SAR405 (10 μ M) for 1h prior to serum recovery, a concentration and
215 incubation time previously shown to fully inhibit Vps34 kinase activity *in vitro* (25). Serum
216 recovery occurred through the removal of EBSS and addition of DMEM (2% HS) for 30min prior
217 to collection. Before collection, myotubes were washed twice in ice-cold PBS, before being
218 scraped into 150 μ L ice-cold sucrose lysis buffer (50 mM Tris, 1 mM EDTA, 1 mM EGTA, 50
219 mM NaF, 5 mM $\text{Na}_4\text{P}_2\text{O}_7 \cdot 10\text{H}_2\text{O}$, 270 mM sucrose, 1 M Triton-X, 25 mM β -glycerophosphate,
220 1 μ M Trichostatin A, 10 mM Nicotinamide, 1 mM 1,4-Dithiothreitol, 1% Phosphatase Inhibitor
221 Cocktail 2 (Sigma), 1% Phosphatase Inhibitor Cocktail 2 (Sigma), 4.8% cOmplete Mini Protease
222 Inhibitor Cocktail; (Roche). Lysates were then immediately frozen in liquid nitrogen and stored
223 at -80°C until analysis. Experiments were conducted in triplicate at 3 separate passage numbers
224 equalling n=9 for statistical analysis.

225 Human primary myoblasts were isolated from 4 patients (age 61 ± 6 yrs, BMI 28.7 ± 0.65 kg/m²,
226 mean \pm SEM) as previously described (23). Cells were passaged at 60% confluency on 0.2%
227 gelatin-coated 100mm culture plates in Hams F10 media (ThermoFisher Scientific,
228 supplemented with 20% FBS and 1% PS) to prevent spontaneous fusion of myoblasts to
229 myotubes, and at passage 3 were seeded onto 6-well plates at a density of 5×10^4 cells/well.
230 Myoblasts were then cultured to 80-90% confluency, at which time media was changed to induce
231 differentiation to myotubes (F10 supplemented with 6% HS and 1% PS). Once myotubes were
232 fully formed (6-10days), experiments were conducted in a similar fashion to those described
233 above for C2C12 myotubes with certain alterations. Baseline conditions for human primary
234 myotubes were ~14h incubation in Hams F10 media (20%FBS, 1%PS) and serum recovery
235 experiments were conducted for 30min in Hams F10 (20%FBS, 1%PS) following ~14h EBSS
236 incubation. All other experimental variables were consistent between C2C12 and human primary
237 experiments and cells were collected in an identical fashion. Experiments were run in triplicate
238 for myotubes isolated from each patient and the mean of these results utilized for statistical
239 analysis.

240 Cell lysates were subsequently homogenised by sonication (3x15s at 50% maximal wattage) and
241 centrifuged at 8000g for 10mins at 40°C to remove insoluble material. Protein content of these
242 lysates was then determined by DC protein assay (BioRad, Hercules, CA, USA.) and samples
243 were diluted to a desired protein concentration in 1x Laemmli sample buffer and boiled at 95°C
244 for 5 minutes to denature proteins.

245 *Immunoblotting*

246 Immunoblotting analysis was conducted as described previously (29). Briefly, equal amounts of
247 protein were loaded into 8-15% polyacrylamide gels and separated by SDS-PAGE. Proteins were
248 then transferred to BioTrace NT nitrocellulose membranes (Pall Life Sciences, Pensacola, FL,
249 USA.) and stained with Ponceau S as a loading control. Membranes were then blocked in 3%
250 skimmed-milk diluted in Tris-buffered Saline with tween (TBST) for 1h at RT. Following
251 washing in TBST, membranes were then incubated overnight in relevant primary antibodies,
252 subsequently washed again and incubated in corresponding HRP-conjugated secondary
253 antibodies (anti-rabbit IgG #7074, Cell Signaling Technologies (CST), Danvers, MA, USA.
254 1:10000). Enhanced chemiluminescence HRP detection kit (Merck-Millipore, Watford, UK.)
255 was used to quantify antibody binding. Each phosphorylated protein visualized was expressed in
256 relation to its total protein content, after each target had been normalized to a loaded control
257 (Ponceau). All primary antibodies utilized for immunoblotting were purchased from CST and
258 diluted at 1:1000 in TBST unless stated otherwise: p70 ribosomal S6 kinase 1 (S6K1, #2708), p-
259 S6K1^{Thr389} (#9205), ribosomal protein S6 (S6, #2217), p-S6^{Ser235/236} (#4858), p-S6^{Ser240/244}
260 (#5364), eukaryotic translation initiation factor 4E-binding protein 1 (4EBP1, #9452, 1:500) and
261 p-4EBP1^{Thr37/46} (#9459).

262 *Statistical analysis*

263 Alterations in enzyme kinase activity, protein-protein colocalization, plasma insulin and plasma
264 leucine concentrations were analysed utilizing a repeated measures analysis of variance
265 (ANOVA) with one within-subject factor (time). Changes in phosphorylation status of proteins
266 in human primary myotubes was also analysed with a repeated measures ANOVA with one
267 within-subject factor (condition). A one-way ANOVA with one between-subject factor
268 (condition) was used to analyse changes in phosphorylation status of proteins in C2C12

269 myotubes. Greenhouse-Geisser corrections were applied to F values if data did not pass
270 Mauchly's test of sphericity. If a significant main effect was found, *post-hoc* analysis was
271 conducted on comparisons determined *a priori* with the Holm-Bonferroni correction for multiple
272 comparisons. Significance for all variables was set at $p < 0.05$ and data are presented as
273 mean \pm SEM unless otherwise stated.

274 **Results**

275 *Blood Analyses*

276 For plasma insulin analysis, physiological results from 7 out of 8 participants were obtained and,
277 as such, statistical analysis was completed on $n=7$. A significant time effect was observed for
278 changes in plasma insulin concentrations ($p < 0.001$), however, following *post hoc* analysis no
279 differences between individual time points were noted ($p > 0.05$, Figure 2A). A significant time
280 effect was also observed for plasma leucine concentrations ($p < 0.001$). Plasma leucine
281 concentrations were elevated above basal levels at 20min post-feeding (0.113 ± 0.006 vs.
282 0.187 ± 0.016 mmol/L, $p = 0.02$, Figure 2B) and remained above baseline (all $p < 0.012$) until
283 160min post-feeding (0.113 ± 0.006 vs. 0.118 ± 0.006 , $p = 0.51$).

284 *Kinase Activity Assays*

285 A significant time effect was observed for S6K1 activity ($p = 0.001$), with S6K1 activity
286 significantly higher 1h post-feeding compared to PRE and 3h post-feeding (1h – $941.3 \pm 164.6\%$
287 of PRE, 3h – $149.6 \pm 23.2\%$ of PRE, $p = 0.003$ & $p = 0.004$ respectively, Figure 2C). Activity of
288 S6K1 also trended toward being greater at 3h post-feeding compared to PRE ($p = 0.07$, Figure
289 2C). A significant time effect was also apparent for AKT activity ($p = 0.05$, Figure 2D). Following
290 *post hoc* analysis, however, no differences in AKT activity between individual time points was

291 apparent (1h – $206.9 \pm 46.6\%$ of PRE, 3h – $118.1 \pm 15.5\%$ of PRE, $p > 0.05$, Figure 2D). Finally, no
292 differences in Vps34 activity were noted at any time point ($p > 0.05$, Figure 2E).

293 *Co-localization*

294 No time effect for mTOR co-localization with LAMP2 (lysosomal marker) was found ($p = 0.347$,
295 Figure 3B) suggesting these proteins are co-localized independently of a nutritional stimulus. A
296 significant time effect was observed for mTOR co-localization with WGA (membrane marker,
297 $p = 0.026$). Following feeding, mTOR-WGA co-localization increased by 17% at 1h before
298 returning to basal values by 3h, however, following *post hoc* analysis, no alterations were
299 significant (PRE – 0.186 ± 0.009 , 1h – 0.212 ± 0.014 , 3h – 0.184 ± 0.009 , PRE vs. 1h $p = 0.090$, 1h
300 vs. 3h $p = 0.067$, Figure 3C). Vps34 co-localization with WGA exhibited a trend toward a time
301 effect ($p = 0.053$) and subsequent *post hoc* analysis revealed that co-localization was greater 1h
302 post-feeding compared to PRE feeding levels (0.347 ± 0.022 vs. 0.273 ± 0.021 , $p = 0.043$, Figure
303 4B), however no other differences were apparent ($p > 0.05$). Finally, there was a significant effect
304 of time observed for mTOR co-localization with Vps34 ($p = 0.045$). Here, following *post hoc*
305 analysis no differences between individual time points were apparent ($p > 0.05$), although a trend
306 toward a greater mTOR-Vps34 co-localization 1h post-feeding compared to 3h was noted
307 (0.347 ± 0.024 vs. 0.315 ± 0.016 , $p = 0.067$, Figure 4C).

308 *In vitro experiments*

309 In C2C12 myotubes, a significant effect of treatment was found for S6K1^{Thr389} phosphorylation
310 ($p < 0.001$, Figure 5A). Here, nutrient/serum withdrawal significantly attenuated S6K1^{Thr389}
311 phosphorylation compared to baseline levels (34% reduction, $p < 0.001$), whereas phosphorylation
312 was elevated by 65% and 50% in serum recovery (SR) and SR+SAR405 treatments respectively

313 (both $p < 0.001$, Figure 5A) with no difference between these two conditions ($p = 0.26$). A
314 treatment effect was also noted for 4EBP1^{Thr37/46} phosphorylation ($p < 0.001$), however subsequent
315 *post hoc* analysis revealed nutrient/serum withdrawal only significantly altered phosphorylation
316 compared to baseline (~28% reduction, $p = 0.015$, Figure 5B). Again, no difference between SR
317 and SR+SAR405 was observed ($p = 0.57$).

318 A significant treatment effect was also noted for both RPS6^{Ser235/236} and RPS6^{Ser240/244}
319 phosphorylation (both $p < 0.001$). RPS6^{Ser235/236} phosphorylation was significantly reduced by
320 nutrient/serum withdrawal (33%, $p < 0.001$, Figure 5C), whereas SR elicited a significant
321 elevation in RPS6^{Ser235/236} phosphorylation above baseline levels (32.7% increase, $p = 0.038$,
322 Figure 5C). A trend toward SR+SAR405 eliciting an elevation in RPS6^{Ser235/236} phosphorylation,
323 compared to baseline, was also observed (29.5% increase, $p = 0.05$) with no difference between
324 the response of this treatment compared to SR ($p = 0.83$). Following *post hoc* analysis of
325 RPS6^{Ser240/244} phosphorylation, only serum/nutrient withdrawal altered phosphorylation status in
326 relation to baseline (18% reduction, $p < 0.001$, Figure 5D). No difference between SR and
327 SR+SAR405 was observed ($p = 0.80$). Representative immunoblots are displayed in Figure 5E.

328 In human primary myotubes, a significant treatment effect was noted for S6K1^{Thr389}
329 phosphorylation ($p < 0.001$). Here, serum/nutrient withdrawal reduced S6K1^{Thr389} phosphorylation
330 by ~70% compared to baseline ($p = 0.026$, Figure 6A). SR and SR+SAR405 both elevated
331 S6K1^{Thr389} phosphorylation above baseline levels (92% & 54%, $p = 0.026$ & 0.035 respectively,
332 Figure 6A). A trend for a greater response in SR, compared to SR+SAR405, was also observed
333 ($p = 0.069$). A treatment effect for 4EBP1^{Thr37/46} phosphorylation was also observed ($p = 0.004$),
334 however, following *post hoc* analysis no differences in 4EBP1^{Thr37/46} phosphorylation between
335 individual treatment conditions was apparent ($p > 0.05$, Figure 6B). Significant treatment effects

336 were also observed for RPS6^{Ser235/236} and RPS6^{Ser240/244} phosphorylation, however *post hoc*
337 analysis for both these variables did not reveal differences between individual treatments
338 ($p > 0.05$, Figures 6C & 6D respectively). Representative immunoblots are displayed in Figure
339 6E.

340 Discussion

341 The class III PI3Kinase, Vps34, has been proposed as a nutrient/amino acid sensitive regulator of
342 mTORC1 activity (4, 10, 22). To examine Vps34 action in human skeletal muscle, we examined
343 changes in Vps34 activity and cellular localization following PRO-CHO ingestion *in vivo* and
344 assessed the effect of Vps34 inhibition on anabolic responses to nutrient availability *in vitro* in
345 C2C12 and human primary myotubes. We observed that PRO-CHO ingestion altered Vps34
346 localization, promoting translocation to the cell periphery and co-localization with mTORC1. Of
347 note, these changes occurred independent of alterations in Vps34 kinase activity. In parallel, our
348 *in vitro* studies demonstrated that the Vps34 specific inhibitor SAR405 did not affect nutrient
349 stimulated activation of mTORC1. Together, these observations suggest a change in Vps34
350 cellular location, rather than an increase in kinase activity, may contribute to mTORC1 nutrient
351 sensing in human skeletal muscle, however, loss of Vps34 activity does not prevent nutrient
352 stimulation of mTORC1 *in vitro*.

353 The finding that PRO-CHO ingestion did not increase Vps34 kinase activity was contrary to our
354 hypothesis and contrasts previous studies (4, 22). Previously, it has been shown that high-
355 frequency electrical stimulation, a potent stimulator of mTORC1 activity, elevated Vps34 kinase
356 activity in rodent skeletal muscle, a response suggested by the authors to be mediated by
357 contraction-induced elevations in intracellular leucine (17). Given the increase in plasma leucine

358 reported in the current study, we would expect our feeding protocol to result in similar increases
359 in intramuscular leucine (1). In human skeletal muscle, there is only one previous study to have
360 assessed Vps34 kinase activity (26). Here, sprint exercise combined with PRO-CHO ingestion
361 did not alter kinase activity, whereas exercise in the fasted state elicited a trend toward elevated
362 activity ~1.5h following the final exercise bout. Importantly, in combination with our findings,
363 this suggests that Vps34 kinase is not solely activated by leucine in human skeletal muscle and
364 may suggest that a contraction stimulus is needed to activate this kinase.

365 In an attempt to further clarify the role of Vps34 in mTORC1 activation in skeletal muscle, we
366 completed *in vitro* experiments in both C2C12 and human primary myotubes, utilising the Vps34
367 specific inhibitor SAR405 (25). In support of our findings *in vivo*, we observed no effect of
368 SAR405 administration on mTORC1 signaling responses to serum recovery in C2C12 or human
369 primary myotubes, suggesting Vps34 kinase activity is not necessary for mTORC1 activation.

370 Recent work from our lab (11, 28), and others (15) suggests that mTORC1 activation in skeletal
371 muscle involves the translocation of mTORC1-lysosome complexes to peripheral regions of the
372 cell (12). Here, we report a similar process by which mTOR-LAMP2 co-localize in the fasted
373 state, prior to mTOR-LAMP2 complex translocation post PRO-CHO ingestion. Vps34 has
374 previously been implicated in mTOR translocation *in vitro*, where it is required for the
375 recruitment of mTOR to lamellipodia (cellular projections of motile cells) in response to insulin
376 stimulation, co-localizing with mTOR in these regions (10). In the current study, we also found
377 Vps34 translocation toward the cell periphery following nutrient provision, with a trend toward a
378 time effect noted for Vps34-WGA co-localization ($p=0.053$). In this context, Vps34-WGA co-
379 localization increased significantly above basal fasted levels 1 hour post-feeding ($p=0.043$)
380 before returning to basal fasted levels 3 hours post PRO-CHO ingestion. Therefore, our

381 observation that Vps34 translocation, and localization with mTORC1, occurs in human skeletal
382 muscle indicates that Vps34 may act as a scaffold for mTORC1 recruitment toward the cell
383 periphery, with an increase in Vps34 kinase activity not required for this process.

384 From the current data it is not possible to conclude whether Vps34 and mTORC1 translocate in
385 tandem or independently before co-localizing, or the physiological relevance of these events in
386 human skeletal muscle. A potential mechanism as to how Vps34 may regulate mTORC1
387 translocation and activation has recently been proposed by Hong and colleagues (13) who
388 suggested that the product of Vps34 kinase activity, PI(3)P, may regulate lysosomal positioning
389 via its receptor, FYCO1 (13). In this model, AAs increase the association between FYCO1 and
390 lysosomes, whereas the ablation of this protein caused the clustering of mTOR-positive
391 lysosomes to perinuclear regions and attenuated mTORC1 activity irrespective of nutrient
392 availability (13). Other potential mechanisms as to how Vps34 may regulate mTORC1 activity
393 include via Tuberous Sclerosis Complex 2 (TSC2) ubiquitination (21) and leucyl t-RNA
394 synthetase (LRS)-regulated mTORC1 activation (34), however each of these processes require
395 further investigation to determine their relevance for mTORC1 activity in skeletal muscle.

396 In conclusion, we report that PRO-CHO ingestion does not increase Vps34 activity in human
397 skeletal muscle, whilst pharmacological inhibition of Vps34 does not prevent nutrient
398 stimulation of mTORC1. However, PRO-CHO ingestion did promote Vps34 translocation to the
399 cell periphery, where Vps34/mTOR co-localize. Therefore, our data suggests that cellular
400 trafficking of Vps34 may result from increased PRO-CHO availability and occur in order to
401 increase Vps34 association with mTOR. Future research studying the effects of resistance
402 exercise, independently or in combination with AA ingestion may be required to fully understand
403 the role of Vps34 in nutrient sensing and skeletal muscle anabolism.

404 **Authors Contributions**

405 N.H. & A.P. conceived the study. J.R.D. Z.S. L.B. & A.P. designed and conducted *in vivo*
406 experiments. N.H. conducted and completed analysis for all *in vitro* experiments. N.H. J.R.D.
407 Z.S. S.J. D.L.H. J.T.M. M.F.O. T.N. & S.W.J. performed analysis. N.H. completed data
408 processing and statistical analysis. N.H. J.R.D. & A.P. drafted the manuscript. All authors
409 approved the final version.

410

411 **References**

- 412 1. **Apro W, Moberg M, Hamilton DL, Eklom B, Rooyackers O, Holmberg HC, Blomstrand E.**
413 Leucine does not affect mechanistic target of rapamycin complex 1 assembly but is required for
414 maximal ribosomal protein s6 kinase 1 activity in human skeletal muscle following resistance
415 exercise. *Faseb j* (2015). doi: 10.1096/fj.15-273474.
- 416 2. **Backer JM.** The intricate regulation and complex functions of the Class III phosphoinositide 3-
417 kinase Vps34. *Biochem J* 473: 2251–2271, 2016.
- 418 3. **Borsheim E, Cree MG, Tipton KD, Elliott TA, Aarsland A, Wolfe RR.** Effect of carbohydrate
419 intake on net muscle protein synthesis during recovery from resistance exercise. *J Appl Physiol* 96:
420 674–678, 2004.
- 421 4. **Byfield MP, Murray JT, Backer JM.** hVps34 is a nutrient-regulated lipid kinase required for
422 activation of p70 S6 kinase. *J Biol Chem* 280: 33076–33082, 2005.
- 423 5. **Dickinson JM, Fry CS, Drummond MJ, Gundermann DM, Walker DK, Glynn EL,**
424 **Timmerman KL, Dhanani S, Volpi E, Rasmussen BB.** Mammalian target of rapamycin
425 complex 1 activation is required for the stimulation of human skeletal muscle protein synthesis by
426 essential amino acids. *J Nutr* 141: 856–862, 2011.
- 427 6. **Drummond MJ, Fry CS, Glynn EL, Dreyer HC, Dhanani S, Timmerman KL, Volpi E,**
428 **Rasmussen BB.** Rapamycin administration in humans blocks the contraction-induced increase in
429 skeletal muscle protein synthesis. *J Physiol* 587: 1535–1546, 2009.
- 430 7. **Dunn KW, Kamocka MM, McDonald JH.** A practical guide to evaluating colocalization in
431 biological microscopy. *Am J Physiol Cell Physiol* 300: C723-42, 2011.
- 432 8. **Gillooly DJ, Simonsen A, Stenmark H.** Cellular functions of phosphatidylinositol 3-phosphate
433 and FYVE domain proteins [Online]. *Biochem J* 355: 249–258, 2001.
434 <https://www.ncbi.nlm.nih.gov/pmc/articles/PMC1221734/pdf/11284710.pdf>.
- 435 9. **Gran P, Cameron-Smith D.** The actions of exogenous leucine on mTOR signalling and amino

- 436 acid transporters in human myotubes. *BMC Physiol* 11: 10, 2011.
- 437 10. **Hirsch DS, Shen Y, Dokmanovic M, Yu J, Mohan N, Elzarrad MK, Wu WJ.** Insulin
438 activation of vacuolar protein sorting 34 mediates localized phosphatidylinositol 3-phosphate
439 production at lamellipodia and activation of mTOR/S6K1. *Cell Signal* 26: 1258–1268, 2014.
- 440 11. **Hodson N, McGlory C, Oikawa SY, Jeromson S, Song Z, Ruegg MA, Hamilton DL, Phillips**
441 **SM, Philp A.** Differential localization and anabolic responsiveness of mTOR complexes in human
442 skeletal muscle in response to feeding and exercise. *Am J Physiol Cell Physiol* 313: C604–c611,
443 2017.
- 444 12. **Hodson N, Philp A.** The Importance of mTOR Trafficking for Human Skeletal Muscle
445 Translational Control [Online]. *Exerc Sport Sci Rev* 47, 2019. [https://journals.lww.com/acsm-](https://journals.lww.com/acsm-essr/Fulltext/2019/01000/The_Importance_of_mTOR_Trafficking_for_Human.8.aspx)
446 [essr/Fulltext/2019/01000/The_Importance_of_mTOR_Trafficking_for_Human.8.aspx](https://journals.lww.com/acsm-essr/Fulltext/2019/01000/The_Importance_of_mTOR_Trafficking_for_Human.8.aspx).
- 447 13. **Hong Z, Pedersen NM, Wang L, Torgersen ML, Stenmark H, Raiborg C.** PtdIns3P controls
448 mTORC1 signaling through lysosomal positioning. *J Cell Biol* 216: 4217–4233, 2017.
- 449 14. **Kim DH, Sarbassov DD, Ali SM, King JE, Latek RR, Erdjument-Bromage H, Tempst P,**
450 **Sabatini DM.** mTOR interacts with raptor to form a nutrient-sensitive complex that signals to the
451 cell growth machinery [Online]. *Cell* 110: 163–175, 2002. [http://ac.els-](http://ac.els-cdn.com/S0092867402008085/1-s2.0-S0092867402008085-main.pdf?_tid=6375041c-87ed-11e5-8ca3-00000aab0f02&acdnat=1447189115_c63136ee9570adfaf0e602858fe83dcb)
452 [cdn.com/S0092867402008085/1-s2.0-S0092867402008085-main.pdf?_tid=6375041c-87ed-11e5-](http://ac.els-cdn.com/S0092867402008085/1-s2.0-S0092867402008085-main.pdf?_tid=6375041c-87ed-11e5-8ca3-00000aab0f02&acdnat=1447189115_c63136ee9570adfaf0e602858fe83dcb)
453 [8ca3-00000aab0f02&acdnat=1447189115_c63136ee9570adfaf0e602858fe83dcb](http://ac.els-cdn.com/S0092867402008085/1-s2.0-S0092867402008085-main.pdf?_tid=6375041c-87ed-11e5-8ca3-00000aab0f02&acdnat=1447189115_c63136ee9570adfaf0e602858fe83dcb).
- 454 15. **Korolchuk VI, Saiki S, Lichtenberg M, Siddiqi FH, Roberts EA, Imarisio S, Jahreis L,**
455 **Sarkar S, Futter M, Menzies FM, O’Kane CJ, Deretic V, Rubinsztein DC.** Lysosomal
456 positioning coordinates cellular nutrient responses. *Nat Cell Biol* 13: 453–460, 2011.
- 457 16. **Ma XM, Blenis J.** Molecular mechanisms of mTOR-mediated translational control [Online]. *Nat*
458 *Rev Mol Cell Biol* 10: 307–318, 2009. <http://dx.doi.org/10.1038/nrm2672>.
- 459 17. **MacKenzie MG, Hamilton DL, Murray JT, Taylor PM, Baar K.** mVps34 is activated
460 following high-resistance contractions. *J Physiol* 587: 253–260, 2009.
- 461 18. **McGlory C, White A, Treins C, Drust B, Close GL, Maclaren DP, Campbell IT, Philp A,**
462 **Schenk S, Morton JP, Hamilton DL.** Application of the [γ - 32 P] ATP kinase assay to study
463 anabolic signaling in human skeletal muscle. *J Appl Physiol* 116: 504–513, 2014.
- 464 19. **McKendry J, Perez-Lopez A, McLeod M, Luo D, Dent JR, Smeuninx B, Yu J, Taylor AE,**
465 **Philp A, Breen L.** Short inter-set rest blunts resistance exercise-induced increases in myofibrillar
466 protein synthesis and intracellular signalling in young males. *Exp Physiol* 101: 866–882, 2016.
- 467 20. **Miller SL, Tipton KD, Chinkes DL, Wolf SE, Wolfe RR.** Independent and combined effects of
468 amino acids and glucose after resistance exercise. *Med Sci Sports Exerc* 35: 449–455, 2003.
- 469 21. **Mohan N, Shen Y, Dokmanovic M, Endo Y, Hirsch DS, Wu WJ.** VPS34 regulates TSC1/TSC2
470 heterodimer to mediate RheB and mTORC1/S6K1 activation and cellular transformation.
471 *Oncotarget* (2016). doi: 10.18632/oncotarget.10469.
- 472 22. **Nobukuni T, Joaquin M, Roccio M, Dann SG, Kim SY, Gulati P, Byfield MP, Backer JM,**
473 **Natt F, Bos JL, Zwartkruis FJT, Thomas G.** Amino acids mediate mTOR/raptor signaling
474 through activation of class 3 phosphatidylinositol 3OH-kinase. *Proc Natl Acad Sci U S A* 102:
475 14238–14243, 2005.

- 476 23. **O’Leary MF, Wallace GR, Bennett AJ, Tsintzas K, Jones SW.** IL-15 promotes human
477 myogenesis and mitigates the detrimental effects of TNF α on myotube development. *Sci Rep* 7:
478 12997, 2017.
- 479 24. **Pasquier B.** SAR405, a PIK3C3/Vps34 inhibitor that prevents autophagy and synergizes with
480 MTOR inhibition in tumor cells. *Autophagy* 11: 725–726, 2015.
- 481 25. **Ronan B, Flamand O, Vescovi L, Dureuil C, Durand L, Fassy F, Bachelot MF, Lambertson
482 A, Mathieu M, Bertrand T, Marquette JP, El-Ahmad Y, Filoche-Romme B, Schio L, Garcia-
483 Echeverria C, Goulaouic H, Pasquier B.** A highly potent and selective Vps34 inhibitor alters
484 vesicle trafficking and autophagy. *Nat Chem Biol* 10: 1013–1019, 2014.
- 485 26. **Rundqvist HC, Lilja MR, Rooyackers O, Odrzywol K, Murray JT, Esbjornsson M, Jansson
486 E.** Nutrient ingestion increased mTOR signaling, but not hVps34 activity in human skeletal
487 muscle after sprint exercise. *Physiol Rep* 1: e00076, 2013.
- 488 27. **Sancak Y, Bar-Peled L, Zoncu R, Markhard AL, Nada S, Sabatini DM.** Ragulator-Rag
489 complex targets mTORC1 to the lysosomal surface and is necessary for its activation by amino
490 acids. *Cell* 141: 290–303, 2010.
- 491 28. **Song Z, Moore DR, Hodson N, Ward C, Dent JR, O’Leary MF, Shaw AM, Hamilton DL,
492 Sarkar S, Gangloff Y-G, Hornberger TA, Spriet LL, Heigenhauser GJ, Philp A.** Resistance
493 exercise initiates mechanistic target of rapamycin (mTOR) translocation and protein complex co-
494 localisation in human skeletal muscle. *Sci Rep* 7: 5028, 2017.
- 495 29. **Stocks B, Dent JR, Ogden HB, Zemp M, Philp A.** Postexercise skeletal muscle signaling
496 responses to moderate- to high-intensity steady-state exercise in the fed or fasted state. *Am J
497 Physiol Endocrinol Metab* 316: E230–E238, 2019.
- 498 30. **Tarnopolsky MA, Pearce E, Smith K, Lach B.** Suction-modified Bergstrom muscle biopsy
499 technique: experience with 13,500 procedures. *Muscle Nerve* 43: 717–725, 2011.
- 500 31. **Wang X, Li W, Williams M, Terada N, Alessi DR, Proud CG.** Regulation of elongation factor
501 2 kinase by p90(RSK1) and p70 S6 kinase. *Embo j* 20: 4370–4379, 2001.
- 502 32. **Witard OC, Jackman SR, Breen L, Smith K, Selby A, Tipton KD.** Myofibrillar muscle protein
503 synthesis rates subsequent to a meal in response to increasing doses of whey protein at rest and
504 after resistance exercise. *Am J Clin Nutr* 99: 86–95, 2014.
- 505 33. **Wolfe RR.** Skeletal muscle protein metabolism and resistance exercise [Online]. *J Nutr* 136:
506 525s–528s, 2006. <http://jn.nutrition.org/content/136/2/525S.full.pdf>.
- 507 34. **Yoon MS, Son K, Arauz E, Han JM, Kim S, Chen J.** Leucyl-tRNA Synthetase Activates Vps34
508 in Amino Acid-Sensing mTORC1 Signaling. *Cell Rep* 16: 1510–1517, 2016.

509

510 **Table Legends**

511 **Table 1.** Summary of Antibodies Used

512

513 **Figure Legends**

514 **Figure 1.** Schematic of Experimental Protocol for Human Trial.

515

516 **Figure 2.** The effect of protein-carbohydrate feeding on plasma insulin and leucine
517 concentrations and enzyme kinase activities. Insulin concentrations (A) are presented as $\mu\text{U/ml}$
518 and Leucine concentrations (B) are presented as mM. Kinase activity of S6K1 (C), AKT (D) and
519 Vps34 (E) are presented as % of PRE. For A & B, Ψ denotes a significant effect of time ($p < 0.05$)
520 and *denotes a significant difference at this time point compared to 0 ($p < 0.05$). For C, D & E
521 *denotes a significant difference at this time point compared to PRE ($p < 0.05$), #denotes a
522 significant difference at this time point compared to 3h ($p < 0.05$) and Ψ denotes a significant
523 effect of time ($p < 0.05$). All values are presented as mean \pm SEM. Data analyzed on SPSS using
524 Repeated Measures ANOVA with Holm-Bonferroni *post hoc* comparisons conducted on
525 Microsoft Excel. Insulin – n=7, Leucine – n=8. Kinase activities – n=8

526

527 **Figure 3.** The effect of protein-carbohydrate ingestion on mTOR-LAMP2 and mTOR-WGA co-
528 localization. Representative images of mTOR (red), LAMP2 (green) and WGA (blue) stains at
529 each time point are provided (A). Quantification of mTOR-LAMP2 (B) and mTOR-WGA (C)
530 co-localization is presented as Pearson's correlation coefficient. Data in B and C are presented as
531 mean \pm SEM. Ψ denotes a significant effect of time ($p < 0.05$). Data analyzed on SPSS using
532 Repeated Measures ANOVA with Holm-Bonferroni *post hoc* comparisons conducted on
533 Microsoft Excel. All analyses – n=8.

534

535 **Figure 4.** The effect of protein-carbohydrate ingestion on mTOR-VPS34 and mTOR-WGA co-
536 localization. Representative images of mTOR (red), VPS34 (green) and WGA (blue) stains at
537 each time point are provided (A). Quantification of VPS34-WGA (B) and mTOR-VPS34 (C) co-
538 localization is presented as Pearson's correlation coefficient. Data in B and C are presented as
539 mean \pm SEM. Ψ denotes a significant effect of time ($p < 0.05$). *denotes a significant differences at
540 this time point compared to PRE ($p < 0.05$). Data analyzed on SPSS using Repeated Measures
541 ANOVA with Holm-Bonferroni *post hoc* comparisons conducted on Microsoft Excel. All
542 analyses – n=8.

543

544 **Figure 5.** The effects of serum/nutrient withdrawal (~14h) and subsequent serum recovery (30
545 min), +/- SAR405, on anabolic signalling in C2C12 myotubes (n=9/group). S6K1^{Thr389} (A),
546 4EBP1^{Thr37/46} (B), RPS6^{Ser235/236} (C) and RPS6^{Ser240/244} (D) phosphorylation were quantified in
547 relation to their total proteins and ponceau staining was used as a loading control. Representative

548 images are also provided (E). Data is presented in relation to baseline as Mean±SEM. *denotes a
549 significant difference in this treatment compared to B (p<0.05). Data analyzed on SPSS using
550 One-Way ANOVA with Holm-Bonferroni *post hoc* comparisons conducted on Microsoft Excel.
551 All analyses – n=9. B = Baseline, SW = Serum Withdrawal & SR = Serum Recovery.

552

553 **Figure 6.** The effects of serum/nutrient withdrawal (~14h) and subsequent serum recovery (30
554 min), +/- SAR405, on anabolic signalling in human primary myotubes (n=4). S6K1^{Thr389} (A),
555 4EBP1^{Thr37/46} (B), RPS6^{Ser235/236} (C) and RPS6^{Ser240/244} (D) phosphorylation were quantified in
556 relation to their total proteins and ponceau staining was used as a loading control. Representative
557 images are also provided (E). Data is presented in relation to baseline as Mean±SEM. *denotes a
558 significant difference in this treatment compared to B (p<0.05). Ψ denotes a significant effect of
559 treatment (p<0.05). Data analyzed on SPSS using Repeated Measures ANOVA with Holm-
560 Bonferroni *post hoc* comparisons conducted on Microsoft Excel. All analyses – n=4. B =
561 Baseline, SW = Serum Withdrawal & SR = Serum Recovery.

562

Table 1.

Primary antibody	Source	Dilution	Secondary antibody	Dilution
Monoclonal anti-mTOR antibody with mouse antigen, isotype IgG γ 1 kappa	Millipore, 05-1592	1:200	Goat anti-mouse IgG γ 1 kappa Alexa@594	1:200
Polyclonal anti-Lamp2 antibody with rabbit antigen, isotype IgG	Abgent, AP1824d	1:100	Goat anti-rabbit IgG(H+L) kappa Alexa@488	1:200
Monoclonal anti-Vps34/PIK3C3 antibody with rabbit antigen, isotype IgG	Cell Signaling Technology #3358	1:20	Goat anti-mouse IgM Alexa@594	1:200
Wheat Germ Agglutinin-350	W11263, Invitrogen	1:20	Alexa Fluor® 350 Conjugated	N/A

Figure 1.

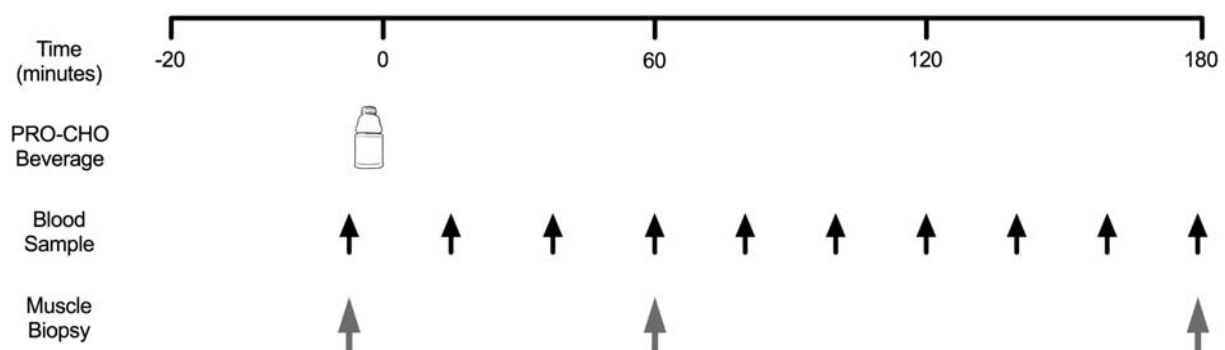


Figure 2.

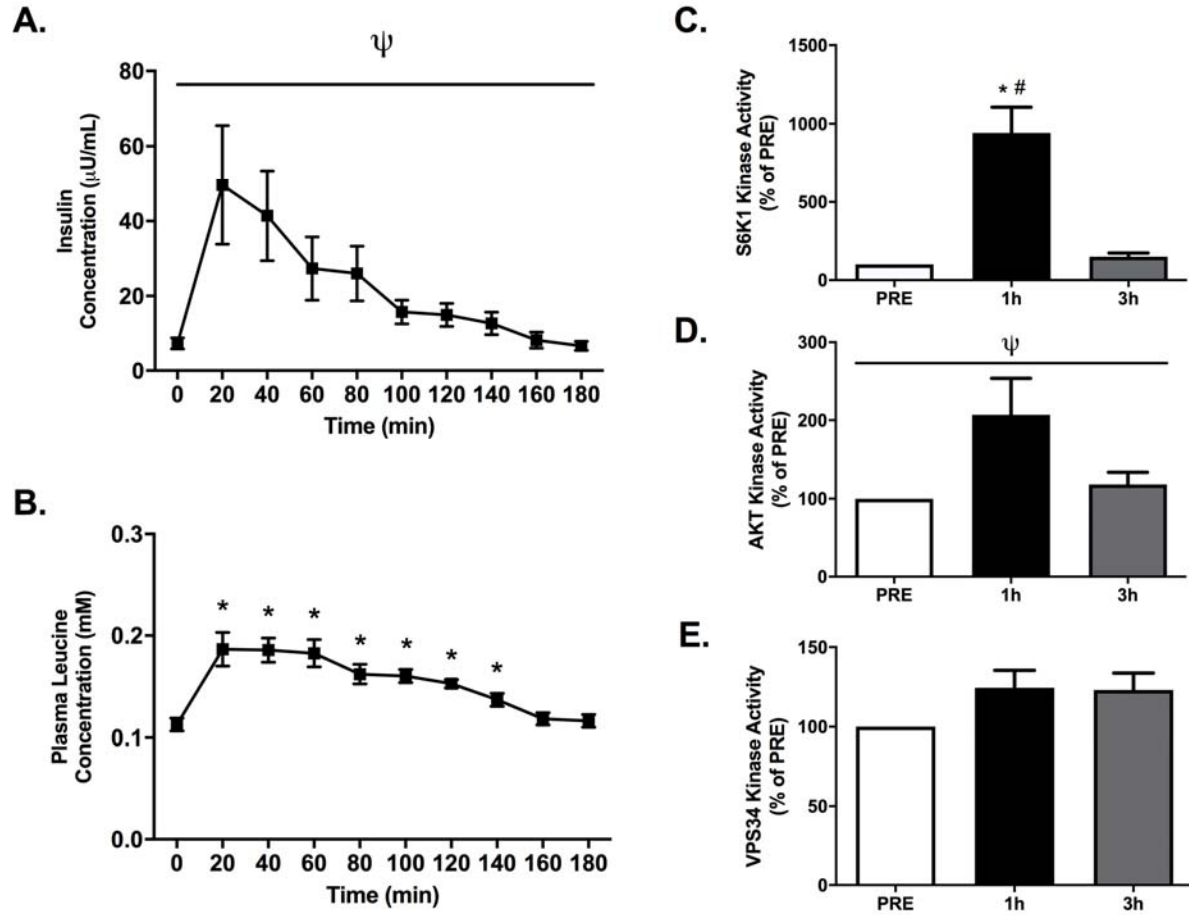


Figure 3.

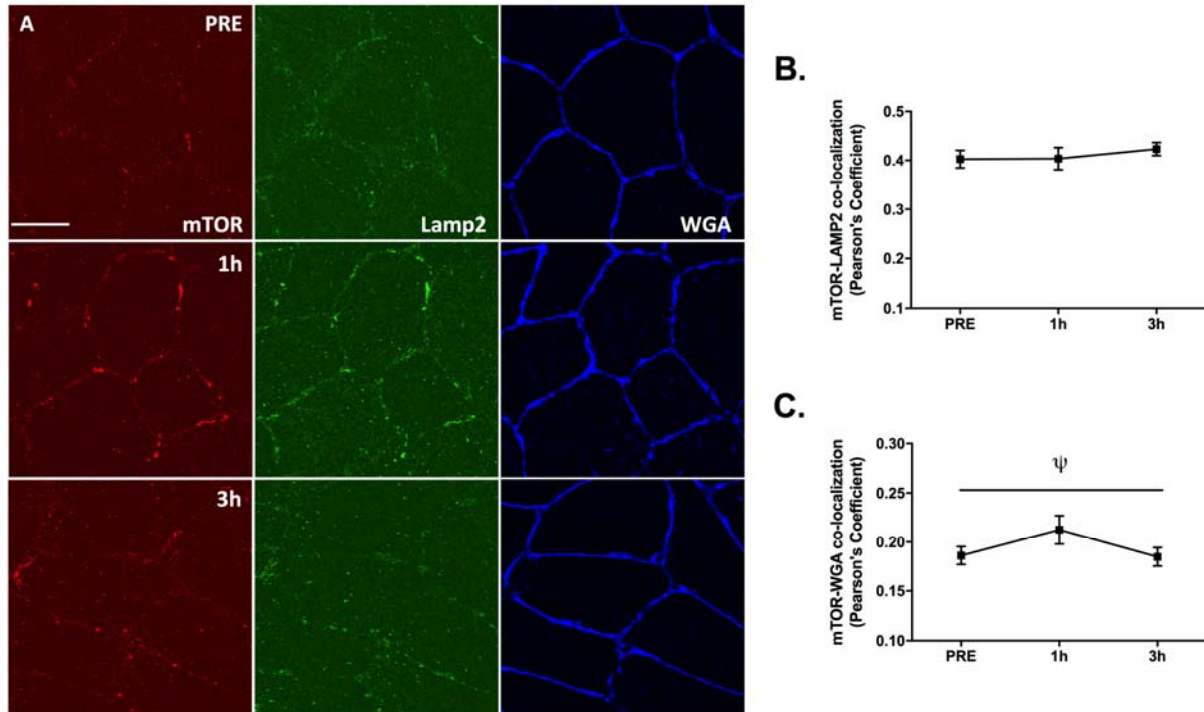


Figure 4.

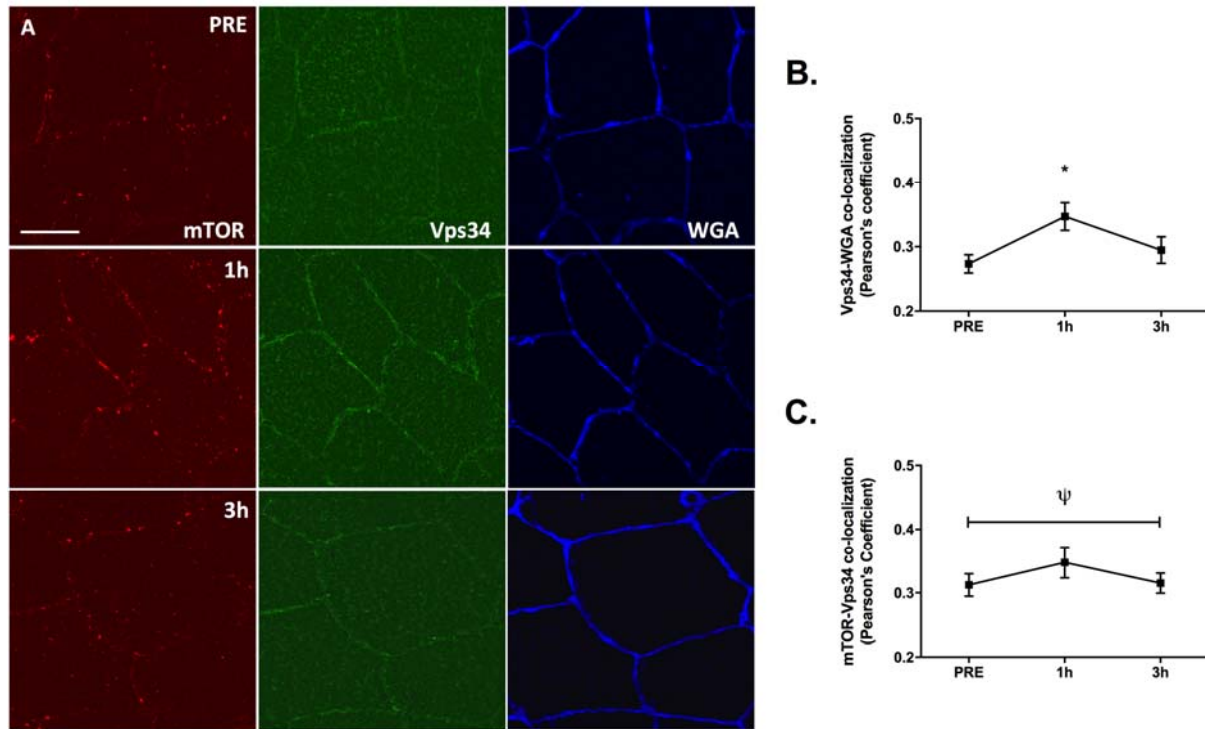


Figure 5.

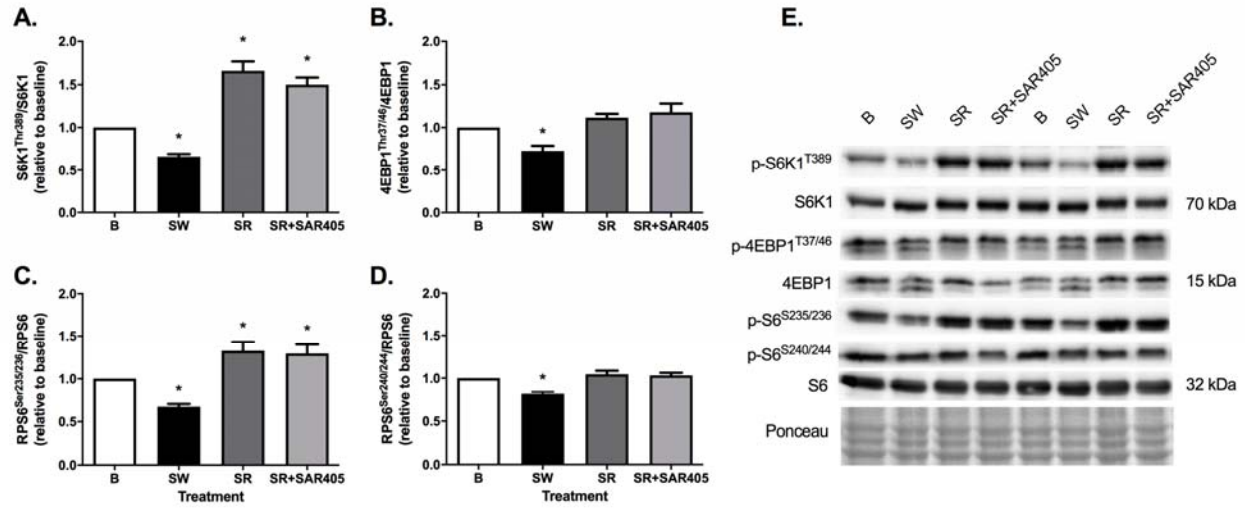


Figure 6.

